free-base porphyrins and metallo-2-methylporphyrins. The best estimate of the allylic coupling constant across the fully delocalized β-β' porphyrin bond (1.00 Hz) was obtained from low-temperature spectra of the N,N'-dideuteriated [N,N'-D_2]-methylporphyrin **2** and was confirmed by measurement of $^4J_{Me,H}$ in the methylbacteriochlorin **4**. The best estimate for the allylic coupling constant across the fully localized β-β' bond that is not involved in the π-electron delocalization pathway was found to be 1.50 Hz. This value was obtained from low-temperature studies on methylnitroporphyrins in which individual tautomers were directly detected. The measured room-temperature $^4J_{Me,H}$ values in a range of substituted porphyrins ((1.02-1.45) $\pm$ 0.03 Hz) were correlated to the π-bond order of the four β-β pyrrolic linkages of the porphyrins. In 2-methyl-5,10,15,20-tetraphenylporphyrin (**2**) ($^4J_{Me,H}$ 1.19 $\pm$ 0.03 Hz), the bond order across the two β-β' pyrrolic bonds involved in the aromatic delocalization pathway in each of the isolated tautomers, **2a** and **2b**, is considerably higher than the bond order in toluene and pyrrole and corresponds to a Pauling bond order of ca. 0.76 or an SCF bond order of ca. 0.66. The bond order across the two β-β' pyrrolic bonds not involved in the delocalization pathway is similar to that found in "pure" double bonds, and these bonds may be regarded as essentially fully localized carbon-carbon double bonds. A similar result was found for a series of deuterioporphyrin dimethyl ester derivatives.

The relatively high bond order between the β-β' pyrrolic carbon atoms within the [18]annulene system is not unreasonable as most aromatic systems other than benzene (e.g., naphthalene) exhibit a range of bond orders. The parameter $^4J_{Me,H}$ also provides an approximate indication of the position of the tautomeric equilibrium. In more complex systems, where coupling information from the inner N-H protons is not available, disturbance of the tautomeric equilibrium can be detected from one measurement at room temperature, which otherwise can only be determined from low-temperature spectra.

The room-temperature $^4J_{Me,H}$ values in methylnitroporphyrins **5-10** range from 1.12 to 1.45 Hz and confirm the values previously obtained for tautomer populations at low temperature, i.e., the nitro group significantly alters the thermodynamic stability of the tautomers. With the establishment of the two extreme values of $^4J_{Me,H}$ in free-base porphyrins, this approach was used to obtain ground-state structural information about bond delocalization between the β-β' pyrrolic positions of metalloporphyrins. For the series of 2-methylporphyrins **15-18** (M = Mg, Zn, Pd, Ni) the $^4J_{Me,H}$ values lie in the range 1.14-1.21 Hz, i.e., a Pauling bond order of ca. 0.76. This finding clearly rules out the possibility that a 16-atom dianion structure with localized double bonds at the four β-β' pyrrolic positions as has been previously been proposed.[8] In order to determine whether the metalloporphyrin structure is best considered as equilibrating 18π-electron tautomers or involves a fully delocalized system, the bond order in two methyl-nitro porphyrins was determined on the free-base and corresponding zinc porphyrins. While β-substitution with the nitro group effects a high degree of bond fixation in free-base porphyrins **8** and **9** by altering the position of the tautomeric equilibrium, no evidence for a parallel result was found in the corresponding zinc(II) metalloporphyrins, **19** and **20**. This result implies that metalloporphyrins are completely delocalized on the NMR time scale; valence bond tautomerism, if present, must involve a very low energy barrier between tautomers.

Acknowledgment. We thank the Australian Research Council for financial support.

Determination of Conformation and Relative Configuration of a Small, Rapidly Tumbling Molecule in Solution by Combined Application of NOESY and Restrained MD Calculations

Michael Reggelin,*,† Holger Hoffmann,‡ Matthias Köck, and Dale F. Mierke

Contribution from the Organisch-Chemisches Institut, Technische Universität München, Lichtenbergstrasse 4, D-8046 Garching, Germany. *Received August 19, 1991*

Abstract: The conformation and relative configuration of seven stereogenic centers in a small, rapidly tumbling molecule have been determined simultaneously in $CDCl_3$ by 2D NOE spectroscopy and restrained MD calculations. Two different methods of evaluating interproton distances from NOESY data were applied and their merits and drawbacks are discussed. The usefulness of the proton detected heteronuclear long range correlation experiment (HMBC) for the assignment of diastereotopic protons is demonstrated. A new approach for the determination of the relative configuration is introduced. By utilizing NOE restraints within molecular dynamic simulations that are larger than the energetic terms responsible for maintaining chirality, the chiral centers can switch and adopt the configuration consistent with the experimental measurements. This approach is illustrated here with the title compound **1** which is extremely well determined by the experimental constraints (58 distance restraints). It adopts a single conformation in $CDCl_3$ solution with structural features similar to corresponding molecular fragments of X-ray structures from similar molecules.

1. Introduction

The determination of the relative and absolute configuration of stereogenic elements in synthetic intermediates, as well as the study of their conformational preferences, is of major importance for both natural product synthesis and the development of new synthetic methods. A deeper insight into the structure and conformation of the species under study is a precondition to predict and optimize the stereochemical outcome of further synthetic transformations.

X-ray crystallographic analysis is without doubt the most secure method to solve the structural problem, but it suffers from the well-known problem of requiring single crystals. Furthermore, the method is principally not suited to analyze conformational preferences of the system *in solution*, which in turn builds the basis for the rational design of new stereoselective transformations.

The method of choice to simultaneously determine configuration and conformation of molecules in solution is obviously NMR spectroscopy, whose capability in this field has been thoroughly

†Present address: Institut für Organische Chemie, Universität Frankfurt, Niederurseler Hang, D-6000 Frankfurt/Main 50, Germany.
‡Schering AG, Müllerstrasse 170-178, D-1000 Berlin 65.

0002-7863/92/1514-3272$03.00/0

demonstrated by impressive studies on oligopeptides[1] and biopolymers.[2] In the field of low-molecular-weight synthetic molecules, the evaluation of magnetic resonance data is often restricted to the analysis of chemical shift and scalar coupling. To solve stereochemical problems, steady state NOE measurements, by means of 1D NOE difference experiments, were used to fix the relative configuration of stereogenic centers. Usually these experiments were carried out under the assumption of a preferred conformation using the NOE only as a means to differentiate between two or more predefined structural possibilities. The attempt to evaluate conformation and configuration of a given chiral molecule simultaneously by the combined application of NMR data (NOE, *J*-coupling) and molecular dynamics[3] calculations, which has been so successful for biopolymers, has not been undertaken in low-molecular-weight systems. An exception in this respect is the recent work of Summers et al., on coenzyme F430 relying on distance geometry and NOESY back-calculations.[4] Indeed there are some obstacles that render such work difficult.

1. The analysis of conformational equilibria in small molecules is often impossible because of the frequent occurrence of high conformational flexibility.

2. External relaxation (leakage) in small molecules (which are in the extreme narrowing limit) is much more effective than for large molecules (spin diffusion limit).[5] Therefore, in the former systems, dipolar interactions, leading to the NOE effect, often compete very inefficiently with other sources of relaxation.

3. In small and medium-sized molecules at current NMR field strengths (ω), the correlation time (τ_c) is often in a range where the NOE effect is of minimum intensity ($\omega\tau_c = 1.12$). Because of the intensity problems caused by the above-mentioned reasons, the realization of intrinsically less sensitive transient NOE experiments, necessary to quantify interproton distances, may become difficult.

However, with the exception of the first point, all these obstacles can be circumvented by the choice of suitable measuring conditions (e.g., temperature, concentration, solvent) and/or NMR experiments (NOESY, ROESY[6]). The almost complete removal of any kind of paramagnetic impurities, including a thorough degassing of the sample, is of utmost importance in this context. In the case of high molecular flexibility, as usually occurs in acyclic systems, the determination of a single conformation is obviously neither possible nor meaningful. Nevertheless, it is very important to recognize this unfavorable situation in order to avoid misinterpretations of the NOE data. The best way to check the presence of such a case is to judge the consistency of the distance data with a single conformation during the conformational study itself. This is why the quantitative evaluation of transient NOE data, as provided, for example, by the 2D NOESY experiment, offers not only the opportunity to analyze configuration and conformation of a given molecule at the same time, but also to prove the validity of the underlying preconditions and assumptions.

For the title compound **1** we have analyzed the conformational preferences of the molecule in $CDCl_3$, as well as the relative configuration of all stereogenic centers by the combined application of the phase sensitive NOESY experiment and restrained molecular dynamics (MD) calculations.

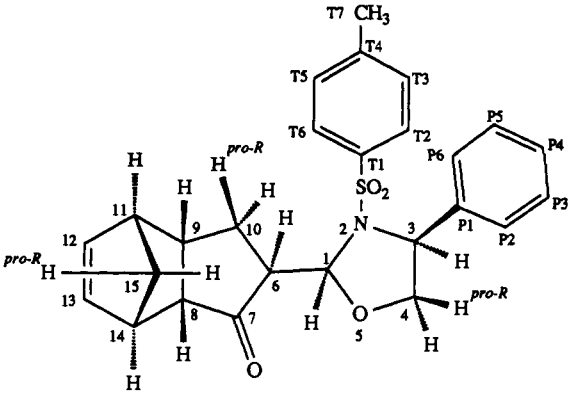

1

Figure 1. Structure of the title compound **1**.

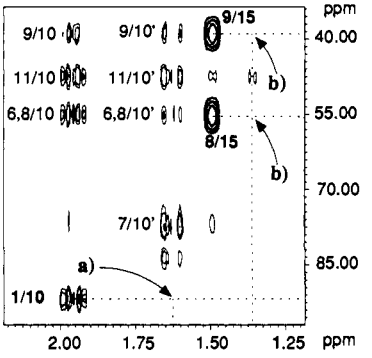

Figure 2. (a) The 500 MHz HMBC spectrum of **1** in $CDCl_3$. The distinct cross peak between C-1 and H-10$^{pro\text{-}R}$ (H-10) as well as the absence of the correlation to H-10$^{pro\text{-}S}$ (H-10') allows for the diastereotopic assignment of these protons. (b) The corresponding region for the diastereotopic proton pair at C-15. Only the *pro-R* proton (δ = 1.50 ppm) gives rise to cross peaks with carbons 8 and 9.

2. Results

Hoppe and co-workers prepared the tricyclic ketone **1** by Diels–Alder reaction as an enantiomerically pure diastereomer in 75% yield and with a diastereoselectivity exceeding 95% ds (Figure 1).[7]

2.1. Assignment of the Proton and Carbon Resonances. The assignment of the nonaromatic protons was possible using the 1D ^{1}H NMR together with a TOCSY spectrum[8] (τ_{mix} = 10 ms), both recorded at 500 MHz. The latter experiment was used as a time saving alternative to the more conventional DQF-COSY. At this stage of the analysis, the unambiguous assignment of the diastereotopic protons at carbons 4, 10, and 15 was not possible.

In order to fix the dihedral angle around the C-1/C-6 bond, which plays a central role in the conformational analysis of the molecule since it defines the relative orientation of the two halves of the molecule, it was necessary to assign all aromatic protons. The decisive experiment in this respect and concerning the problem of the diastereotopic assignments was the proton detected heteronuclear long range correlation (HMBC)[9] in combination with the proton detected ^{1}H,^{13}C shift correlation (HMQC).[10]

Starting with the proton shift of H-3 (4.68 ppm), the $^3J_{CH}$ coupling leads to a cross peak in the HMBC at δ = 126.86 ppm which corresponds to the resonances of the carbon atoms P2/P6. The chemical shift of the protons bound to these carbons can now be taken from the HMQC. The other possible correlation ($^2J_{CH}$),

(1) Kessler, H.; Loosli, H.-R.; Oschkinat, H. *Helv. Chim. Acta* **1985**, *68*, 661–681.
(2) (a) Wüthrich, K. *NMR of Proteins and Nucleic Acids*; John Wiley: New York, 1986. (b) Wagner, G. *Prog. Nucl. Magn. Reson. Spectrosc.* **1990**, *22*, 101–139.
(3) (a) Kaptein, R.; Zuiderweg, E. R. P.; Scheek, R. M.; Boelens, R.; van Gunsteren, W. F. *J. Mol. Biol.* **1985**, *182*, 179–182. (b) Brünger, A. T.; Karplus, M. *Acc. Chem. Res.* **1991**, *24*, 54–61.
(4) (a) Won, H.; Olson, K. D.; Wolfe, R. S.; Summers, M. F. *J. Am. Chem. Soc.* **1990**, *112*, 2178–2184. (b) Olson, K. D.; Won, H.; Wolfe, R. S.; Hare, D. R.; Summers, M. F. *J. Am. Chem. Soc.* **1990**, *112*, 5884–5886.
(5) Neuhaus, D.; Williamson, M. P. *The Nuclear Overhauser Effect in Structural and Conformational Analysis*; VCH Publishers: New York, 1989.
(6) (a) Bothner-By, A. A.; Stephens, R. L.; Lee, J.; Warren, C. D.; Jeanloz, R. W. *J. Am. Chem. Soc.* **1984**, *106*, 811–813. (b) Bax, A.; Davis, D. G. *J. Magn. Reson.* **1985**, *63*, 207–213. (c) Kessler, H.; Griesinger, C.; Kerssebaum, R.; Wagner, K.; Ernst, R. R. *J. Am. Chem. Soc.* **1987**, *109*, 607–609.
(7) Hoppe, D.; Hoffmann, H. Manuscript in preparation.
(8) (a) Braunschweiler, L.; Ernst, R. R. *J. Magn. Reson.* **1983**, *53*, 521–528. (b) Davies, D. G.; Bax, A. *J. Am. Chem. Soc.* **1985**, *107*, 2820–2821. (c) Edwards, M. W.; Bax, A. *J. Am. Chem. Soc.* **1986**, *108*, 918–923.
(9) (a) Bax, A.; Summers, M. F. *J. Am. Chem. Soc.* **1986**, *108*, 2093–2094. (b) Bax, A.; Marion, D. *J. Magn. Reson.* **1988**, *78*, 186–191.
(10) Bax, A.; Subramanian, S. *J. Magn. Reson.* **1986**, *67*, 565–569.

Table I. Proton and Carbon Chemical Shifts and Proton, Proton Coupling Constants in 1

position	δ_H (ppm)	δ_C (ppm)	position	δ_H (ppm)	δ_C (ppm)	protons	J (Hz)
1	5.18	91.72	$15^{pro\text{-}S}$	1.37	52.12	1,6	2.9
3	4.68	61.22	P1		139.51	$3,4^{pro\text{-}R}$	2.4
$4^{pro\text{-}R}$	4.05	72.47	P2	7.41	126.86	$3,4^{pro\text{-}S}$	6.7
$4^{pro\text{-}S}$	3.56	72.47	P3	7.36	128.46	$4^{pro\text{-}R},4^{pro\text{-}S}$	9.0
6	2.90	54.97	P4	7.30	127.76	$6,10^{pro\text{-}R}$	10.0
7		219.6	P5	7.36	128.46	$6,10^{pro\text{-}S}$	10.4
8	2.90	55.27	P6	7.41	126.86	8,9	8.7
9	2.77	38.95	T1		133.34	8,14	4.6[a]
$10^{pro\text{-}R}$	1.96	23.47	T2	7.71	128.20	$9,10^{pro\text{-}R}$	10.0
$10^{pro\text{-}S}$	1.63	23.47	T3	7.34	130.04	$9,10^{pro\text{-}S}$	2.4
11	2.99	47.51	T4		144.50	9,11	4.2
12	6.29	135.1	T5	7.34	130.04	$10^{pro\text{-}R},10^{pro\text{-}S}$	14.1
13	6.12	136.0	T6	7.71	128.20	11,12	3.0
14	3.23	47.80	T7	2.45	21.60	$11,15^{pro\text{-}R}$	1.8
$15^{pro\text{-}R}$	1.50	52.12				$11,15^{pro\text{-}S}$	1.6
						12,13	5.7
						13,14	3.0
						$14,15^{pro\text{-}R}$	1.8
						$14,15^{pro\text{-}S}$	1.6
						$15^{pro\text{-}R},15^{pro\text{-}S}$	8.3

[a] Uncertain, because of poor resolution of the H-14 resonance and overlap of the H-8 resonance.

also visible in the HMBC, leads to the identification of the quaternary carbon P1, which in turn has, as expected, no correlation in the HMQC. In the long range correlation, on the other hand, this carbon interacts via $^3J_{CH}$ coupling with the meta protons P3/P5, leading to their identification.

The assignments of the ^1H and ^{13}C resonances in the *p*-toluenesulfonyl part of the molecule were performed in an analogous manner starting from the *p*-methyl group. The chemical shift data are compiled in Table I.

In order to assign the methylene protons at the carbons 10 and 15 diastereotopically, we exploited the dependence of the transfer amplitude of the HMBC experiment[11] from the magnitude of the heteronuclear long range coupling ($^3J_{CH}$), which in turn is a function of the corresponding dihedral angle.[12]

In the HMBC spectrum only one of the two possible $^3J_{CH}$ correlations from C-1 (δ = 91.72 ppm) to the diastereotopic proton pair at C-10 (δ = 1.96 ppm) is visible (Figure 2a). This observation is consistent with a syn- or antiperiplanar arrangement of the two interacting nuclei. Model studies show that only the *pro-R* proton can adopt a synperiplanar orientation, whereas for the other diastereotopic proton none of the two possibilities can be realized without considerable strain. Similar arguments hold for the assignment of the C-15 methylene group: the only detectable long range correlations exist between C-atoms 8 and 9 at δ = 55.27 ppm and δ = 38.95 ppm, respectively, and the *pro-R* proton (δ = 1.50 ppm) at C-15 which, because of the rigid nature of the tricyclic system places it unambiguously in the antiperiplanar position (Figure 2b). For the second proton (H-$15^{pro\text{-}S}$), enclosing a dihedral angle of about 60° with C-9 and C-8, no cross peak can be detected.

The remaining diastereotopic pair at C-4 is not as easy to assign as in the two cases just described. The potential flexibility of this portion of the molecule, in combination with the double maximum character of the Karplus relation, renders the analysis difficult. For these reasons additional information from the NOE data was necessary to complete the diastereotopic assignment.

2.2. Extraction of Conformationally Relevant Parameters. The determination of proton, proton coupling constants was achieved by the analysis of the 1D ^1H-NMR together with an E.COSY spectrum,[13] both recorded at 500 MHz (Table I). In order to calculate the interproton distances, two different methods were applied. The first, more conventional approach is based on the analysis of a series of NOESY spectra using different mixing times, whereas the second one exploits the distance information available from the intensity ratio of cross and diagonal peaks in these spectra.[14] The main advantage of the second method is that it is theoretically independent from the initial rate approximation.

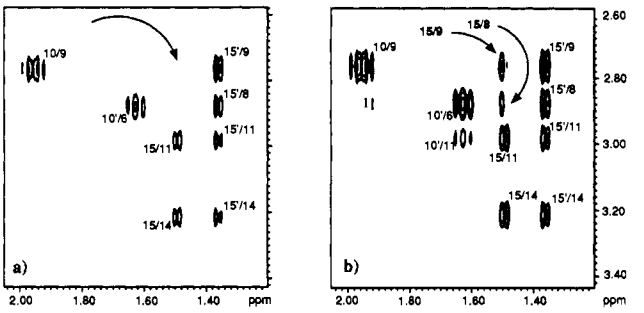

Figure 3. (a) The 500 MHz NOESY spectrum of **1** with τ_{mix} = 800 ms. No cross peaks due to multispin effects are visible in the region indicated by the arrow. (b) After raising τ_{mix} to 1200 ms, two additional cross peaks appear due to three spin effects involving magnetization transfer from H-8 and H-9 to H-$15^{pro\text{-}R}$ (H-15 in the figure) via H-$15^{pro\text{-}S}$ which is close in space with H-8 and H-9 (271 pm and 251 pm, respectively).

2.2.1. Distances from Cross Peak Amplitudes in NOESY Spectra. For the realization of the first approach, eight NOESY spectra using different mixing times (150, 200, 300, 500, 600, 800, 1200, and 2000 ms) were recorded at 500 MHz. As expected for a small molecule, only positive NOE effects are detected up to a mixing time of 800 ms. Beyond this, multispin effects leading to cross peaks with inverted phase occur which in turn render their identification unproblematic (Figure 3).

After volume integration of all cross peaks in the NOESY spectra, excluding the last two mixing times (1200 and 2000 ms), the intensity data were calibrated using the two geminal protons at C-4, assuming their distance to be 178 pm. The validity of the assumption (isolated spin pair approximation, ISPA),[15] underlying the procedure described above, was checked in a 2-fold manner. The mixing time dependence of all cross peak intensities has been monitored graphically to be sure that the linear approximation holds for all dipolar interactions for quantification. Furthermore, for individual cross peaks only those mixing times leading to identical distances were taken into account. This procedure relies on the fact that, within the linear approximation,

(11) (a) Kessler, H.; Gehrke, M.; Griesinger, C. *Angew. Chem., Int. Ed. Engl.* **1988**, *27*, 490–536. (b) Hofmann, M.; Bermel, W.; Gehrke, M.; Kessler, H. *Magn. Reson. Chem.* **1989**, *27*, 877–886.

(12) (a) Wasylishen, R.; Schaefer, T. *Can. J. Chem.* **1973**, *51*, 961–973. (b) Aydin, R.; Loux, J.-P.; Günther, H. *Angew. Chem., Int. Ed. Engl.* **1982**, *21*, 449.

(13) Griesinger, C.; Sørensen, O. W.; Ernst, R. R. *J. Am. Chem. Soc.* **1985**, *107*, 6394–6396.

(14) Esposito, G.; Pastore, A. *J. Magn. Reson.* **1988**, *76*, 331–336.

(15) Borgias, B. A.; Gochin, M.; Kehrwood, D. J.; James, T. L. *Prog. Nucl. Magn. Reson. Spectrosc.* **1990**, *22*, 83–100.

Table II. Interproton Distances from NOESY and MD Calculations

diagonal peak	cross peak	distance (pm)[a]	distance (pm)[b]	distance (pm)[c]	diagonal peak	cross peak	distance (pm)[a]	distance (pm)[b]	distance (pm)[c]
T2, T6	H-6		338	370	H-1	H-4^{pro-R}	444	367	386
H-6	T2, T6	330			H-4^{pro-R}	H-1	445		
H-10^{pro-S}	P2, P6	310	308	433	H-1	H-3	342	319	355
P2, P6	H-10^{pro-S}				H-3	H-1	343		
P2, P6	H-10^{pro-R}		289	332	H-3	H-4^{pro-S}	230	231	223
H-10^{pro-R}	P2, P6	279			H-4^{pro-S}	H-3	229		
T3, T5	T7		224	299	H-3	H-4^{pro-R}	290	288	286
T7	T3, T5	217			H-4^{pro-R}	H-3	290		
P3, P5	H-10^{pro-R}		390	470	H-4^{pro-R}	H-10^{pro-R}	325	321	338
H-10^{pro-R}	P3, P5	323			H-10^{pro-R}	H-4^{pro-R}	321		
P3, P5	H-10^{pro-S}		418	555	H-4^{pro-R}	H-8	364	359	438
H-10^{pro-S}	P3, P5	348			H-8	H-4^{pro-R}	363		
H-12	H-15^{pro-R}	339	360	349	H-4^{pro-R}	H-4^{pro-S}	178	178	179
H-15^{pro-R}	H-12	346			H-4^{pro-S}	H-4^{pro-R}	178		
H-12	H-10^{pro-S}	273	284	304	H-14	H-15^{pro-S}	266	270	268
H-10^{pro-S}	H-12	287			H-15^{pro-S}	H-14	266		
H-13	H-15^{pro-R}	337	358	349	H-14	H-15^{pro-R}	258	262	264
H-15^{pro-R}	H-13	350			H-15^{pro-R}	H-14	260		
H-13	H-10^{pro-S}	457	469	444	H-11	H-10^{pro-R}	457	379	371
H-10^{pro-S}	H-13	490			H-10^{pro-R}	H-11	455		
H-12	H-9	428	447	429	H-11	H-10^{pro-S}	280	281	300
H-9	H-12	440			H-10^{pro-S}	H-11	289		
H-12	H-6	288	312	358	H-11	H-15^{pro-R}	259	262	265
H-6	H-12	295			H-15^{pro-R}	H-11	260		
H-12	H-11	258	270	268	H-11	H-15^{pro-S}	270	271	268
H-11	H-12	263			H-15^{pro-S}	H-11	268		
H-13	H-6	287	306	363	H-8	H-15^{pro-S}	252	254	270
H-6	H-13	299			H-15^{pro-S}	H-8	250		
H-13	H-14	257	273	269	H-6	H-10^{pro-S}	231	232	230
H-14	H-13	265			H-10^{pro-R}	H-6	229		
H-12	H-14	446	461	429	H-6	H-10^{pro-R}	290	266	297
H-14	H-12	453			H-10^{pro-R}	H-6	287		
T2, T6	H-3		249	492	H-9	H-15^{pro-S}	243	242	251
H-3	T2, T6	246			H-15^{pro-S}	H-9	239		
T2, T6	H-1		248	382	H-9	H-10^{pro-S}	296	283	287
H-1	T2, T6	245			H-10^{pro-S}	H-9	304		
P2, P6	H-4^{pro-R}		279	345	H-9	H-10^{pro-R}	227	227	225
H-4^{pro-R}	P2, P6	273			H-10^{pro-R}	H-9	224		
P2, P6	H-3		282	304	H-14	H-8	243	250	262
H-3	P2, P6	275			H-8	H-14	245		
P3, P5	H-4^{pro-R}		379	528	H-11	H-9	245	253	252
H-4^{pro-R}	P3, P5	367			H-9	H-11	247		
P3, P5	H-3		347	509	H-10^{pro-R}	H-10^{pro-S}	179	182	174
H-3	P3, P5	367			H-10^{pro-S}	H-10^{pro-R}	186		
H-1	H-10^{pro-R}	347	348	372	H-15^{pro-R}	H-15^{pro-S}	187	185	178
H-10^{pro-R}	H-1	344			H-15^{pro-S}	H-15^{pro-R}	185		
H-1	H-6	231	234	253	T2, T6	H-4^{pro-S}		386	588
H-6	H-1	231			H-4^{pro-S}	T2, T6	383		
H-1	H-4^{pro-S}	258	260	308	H-1	H-10^{pro-S}	463	442	414
H-4^{pro-S}	H-1	258			H-10^{pro-S}	H-1	476		
					H-3	H-10^{pro-R}	459	455	411
					H-10^{pro-R}	H-3	453		

[a] Distances from the intensity ratio method. Those NOEs where the diagonal could not be integrated are left blank. [b] Distances from the analysis of the cross peak intensities. [c] Distances from the MD calculation.

the ratio between the amplitude of a cross peak and the amplitude of the reference peak has to be constant irrespective of the mixing time. This way of analyzing NOESY data is a handy equivalent to the much more demanding method using NOE buildup rates. All distance data derived in this manner, together with the distances from the intensity ratio method (see later) are compiled in Table II.

2.2.2. Distances from the Intensity Ratio Method. From the ratio of cross and diagonal peak intensities (a_{AB} and a_{AA}, respectively) in NOESY spectra it is possible to describe the internuclear distance r as follows:[14]

$$r = \left\{ \frac{-2q\tau_{mix}}{\ln\left[\dfrac{a_{AA} + a_{AB}}{a_{AA} - a_{AB}}\right]} \left(\frac{6\tau_c}{1 + 4\omega^2\tau_c^2} - \tau_c \right) \right\}^{1/6} \quad (1)$$

The correlation time τ_c, necessary for the application of eq 1, was calculated from (1) again using the known distance between the geminal proton pair H-4^{pro-R} and H-4^{pro-S}. The main advantage of this alternative approach to interproton distances is its independence from the initial rate approximation, although this is only true for two isolated spin $^1/_2$ nuclei. The method offers the opportunity to obtain all the distance data from a single NOESY spectrum, recorded at a value of τ_{mix}, where the cross peaks have significant amplitudes but no multispin effects occur. The derived distances from the NOESY with τ_{mix} = 600 ms and $\tau_c = 3.56 \cdot 10^{-11}$ s are compiled in Table II.

2.3. Conformation and Relative Configuration of 1 in $CDCl_3$. The energy minimizations and molecular dynamics simulations were carried out with the Discover (BIOSYM) program.[16] The starting structure was built using the Insight program. To invert selected centers of chirality, a forcing potential was placed on the selected torsion with a large force constant of 50 kcal/mol·Å^2; energy minimization then produces the structure with the desired

(16) Hagler, A. T. *The Peptides*; Udenfriend, S., Meienhofer, J., Hruby, V., Eds.; Academic Press: Orlando, FL, 1985; Vol. 7, pp 214–296.

Table III. Additional Potential Energy Parameters Used in MD Simulations of 1

bonds[a]		equil Å	K (kcal·mol^{-1}·Å^{-2})
s	o	1.43	100.0
s	n	1.62	100.0

angles[a,b]			equil (deg)	K (kcal·mol^{-1}·deg^{-2})
cp	cp	s	120	90.0
cp	s	o	107	50.0
n	c	o	103	50.0
n	c	cp	116	50.0
s	n	c	118	50.0
cp	s	n	107	50.0
o	s	o	120	50.0
o	s	n	107	50.0

torsion[c]				phase	K (kcal·mol^{-1})	n
cp	cp	s	n	0.0	0.0	3
cp	s	n	c	0.0	7.0	3

[a] Using the equation K(value − equil)^2. [b] cp, aromatic carbon. [c] Using the equation K[1 + cos (n·value − phase)].

chirality. The parameters for the energetic description of the sulfonamide moiety are undefined in commonly utilized force fields.[17] For these undefined parameters, the equilibrium values were set to those from X-ray structures of related compounds containing these molecular features[18] and the force constants approximated from standard literature values of related structures.[19] These parameters are listed in Table III. All of the other parameters are those standardly used.[16,17] All computer simulations were carried out in vacuo on Silicon Graphics 4D/240SX and 4D/70GTB computers.

The distance restraints were derived from the NOEs as described above (Table II). The upper and lower distance bounds were set to plus and minus 5% of the calculated distances, respectively. This small variation allows for some error in the measurement of the intensity of cross peaks and conversion to distances. Restraints involving the methyl group were applied to the average position of the three protons with the addition of 100 pm to the upper bound. All distance restraints involving methylene protons were diastereotopically assigned.

The NOE restrained molecular dynamics simulations were carried out with a time step of 1.0 fs for a duration of 100 ps. The atomic velocities were randomly applied following a Boltzmann distribution about the center of mass to obtain a temperature of 500 K, and the system was allowed to come to equilibrium for 5 ps. A skewed biharmonic constraining function was used for the NOE restraints; maximum forces of 50 and 5 kcal/mol·Å^2 were used for the lower and upper distance restraints, respectively. During the molecular dynamics, structures were taken at regular intervals and completely energy minimized using a quasi-Newton–Raphson minimizer[20] until the derivatives were less than 0.01 kcal/mol·Å.

One MD simulation was carried out starting with the (8*R*,6*S*,1*S*,3*S*,9*R*,11*R*,14*S*) (exo) structure. During the simulation, after approximately 5 ps, the structure reversed chirality at the bridgehead positions 8 and 9, thus establishing the configuration of the endo attack. The change in chirality is caused by the application of the NOE restraints; with a large NOE restraint force constant (20 kcal/mol·Å^2), the NOEs are energetically more important than the angle and torsion energies that

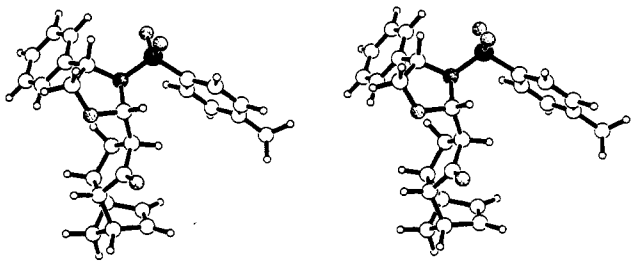

Figure 4. Stereoplot of the conformation of 1 as deduced from the rMD calculations. The sulfur atom is filled, the oxygens are partly stipled, and the nitrogen is stipled.

Table IV. Selected Dihedrals from the rMD Simulation of 1 and the X-ray Structure of 2[a]

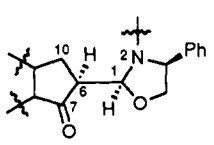

1

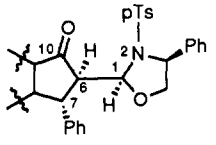

2

torsion	rMD (1) (deg)	X-ray (2) (deg)
N2-C1-C6-C10	−44	−65
N2-C1-C6-C7	−164	175
N2-C1-C6-H6	76	53
H1-C1-C6-H6	−47	−65

[a] The torsions are defined by using a numbering for 2 which is consistent with the numbering used for 1.

maintain the chirality. The NOE restraint energy is 150 kcal/mol compared with an energy of 60 kcal/mol for the angle and torsion restraining term. Once the chirality is modified, the angle and torsion as well as the NOE restraints are fulfilled. The largest deviation was observed for NOEs involving aromatic protons, e.g., T2,T6. Since these protons are identical on the NMR time scale, a correction factor of 210 pm was added to the upper bound of the distance restraint (Table II). An approach somewhat similar to this has been described as "floating chirality,"[21] used to help in the assignment of methylene and methyl protons in proteins.[22] The floating chirality technique uses a drastic reduction of the force constant of the three angles involving the chiral center. Then during the simulation, the NOEs can direct the proper assignment of the protons. Here, we use NOE force constants that are large enough to render the energy term to maintain the chirality negligible. This is an important finding. Without such an approach, each of the possible diastereomers, here 16 structures (2^4), would have to be examined with NOE restrained MD simulations.[23]

To gain some insight into the NOEs that are important in the development of the correct relative configuration, two additional simulations were run with reduced NOE force constants (10 kcal/mol·Å^2) avoiding the inversion of configuration at the bridgehead positions in the exo structure. The simulation starting with the endo adduct had a much smaller NOE restraint energy compared with the simulation with the exo configuration (37 and 96 kcal/mol, respectively). Two NOEs have particularly high restraint energy. In the structure of the exo product the distance between proton 9 and 15$^{pro\text{-}S}$ is much larger (341 pm) than determined experimentally (242 pm). In addition, the distance between H-9 and H-12 in this structure is 210 pm, while a distance greater than 400 pm is derived from the NOEs. These distances are satisfied within the structure with the correct stereochemistry

(17) (a) Weiner, S. J.; Kollman, P. A.; Case, D. A.; Chandra Singh, U.; Ghio, C.; Alagona, G.; Profeta, S.; Weiner, P. *J. Am. Chem. Soc.* **1984**, *106*, 765–784. (b) Momany, F. A.; McGuire, R. F.; Burgess, A. W.; Scheraga, H. A. *J. Phys. Chem.* **1975**, *79*, 2361–2381. (c) van Gunsteren, W. F.; Berendsen, H. J. C. Groningen Molecular Simulation (GROMOS) Library Manual; Biomos B. V.: Nijenborgh, 16, NL 9747 AG Groningen; pp 1–229.

(18) (a) Hoffmann, H. Ph.D. Thesis, Kiel, 1990. (b) Herbst, R.; Berger, B.; Dyrbusch, M.; Egert, E. Manuscript in preparation.

(19) (a) Hargittai, M.; Hargittai, I. *J. Mol. Struct.* **1974**, *20*, 283–292. (b) Allinger, N. L.; Kao, J. *Tetrahedron* **1976**, *32*, 529–536.

(20) Fletcher, R. *Practical Methods of Optimization*; John Wiley: New York, 1980; Vol. 1.

(21) Holak, T. A.; Gondol, D.; Otlewski, J.; Wilusz, T. *J. Mol. Biol.* **1989**, *210*, 635–648.

(22) Güntert, P.; Braun, W.; Billeter, M.; Wüthrich, K. *J. Am. Chem. Soc.* **1989**, *111*, 3997–4004.

(23) The rMD calculation on the C-6 epimer (6*R*) leads to the same relative configuration, although the NOE force constant necessary to invert the chirality at this center was much higher (80 kcal/mol·Å^2) than those causing the exo–endo conversion.

(Table II). A stereoplot of the average structure of **1** from the MD, energy minimized, is shown in Figure 4.

The average of selected torsions defining the relative orientation of the heterocycle and the tricyclic ring system obtained by the MD simulation of the endo compound **1** (with reduced NOE force constants) together with the corresponding torsions of the related structure **2** from X-ray[18] analysis are listed in Table IV.

The most important result that can be deduced from the data in Table IV is the reproduction of the staggered conformation around the C-1/C-6 bond found in the X-ray structure of **2**. This is true irrespective of the inversion of the configuration at C-6 in the latter compound. The observed deviation of ca. 20° of all torsions may be the consequence of an underestimation of the H-1/H-6 distance. Because of the r^{-6} dependence of the cross relaxation rate, even small variations of the internuclear vector caused by conformational flexibility will bias its value toward short distances.

3. Conclusions

The application of transient NOE experiments (e.g., NOESY) is a precondition for the evaluation of quantitative distance data. The time consuming collection of many NOESY spectra with different mixing times can be avoided in the case of minor spectral overlap of the diagonal peaks. In this case, a single NOESY provides all the distance data needed with almost the same precision as the NOE build-up method (Table II). Assuming a strongly preferred conformation of the molecule in solution, it should be possible to derive this conformation and the relative configuration of all its potential stereogenic elements. The latter task is conveniently performed by restrained MD calculations using NOE restraint force constants overriding the angle and torsion energies maintaining the chirality. This approach seems to be very promising especially for the study of compounds whose structures are expected to be different in solution and solid state. Polar organometallic compounds are obvious candidates in this respect, and the usefulness of the above-described methodolgy in the field of these important class of compounds is currently under investigation.

4. Experimental Details

Measurement Conditions. General. All NMR spectra were recorded at 300 K on a Bruker AMX500 spectrometer ($\nu_0(^1H)$ = 500.13 MHz; $\nu_0(^{13}C)$ = 125.75 MHz) equipped with a Bruker Aspect X32 computer. All spectra were recorded with quadrature detection in both dimensions; TPPI[24] was used in F_1. The spectra were processed on a Bruker Aspect X32 computer. All information about sizes and data points of the spectra is given in real points. A sealed sample containing 29 mg/0.3 mL of **1** in degassed $CDCl_3$ was used for all measurements, leading to an overall concentration of 210 mmol/L.

1. 1D ^{1}H NMR Spectrum: size, 16K; sweep width, 5050.50 Hz; pulse length, 9.0 μs (ca. 82° pulse); relaxation delay, 2.0 s; 128 acquisitions; single zero-filling.

2. 1D ^{13}C NMR Spectrum: size, 32K; sweep width, 29 411.80 Hz; pulse length, 6.0 μs (ca. 60° pulse); relaxation delay, 3 s; 20 000 acquisitions; single zero-filling (measuring time, 19 h 47 min).

3. E.COSY Spectrum: sequence; D_1–90°–t_1–90°–D_2–90°–t_2, (phase cycling for three spin E.COSY was applied according to the literature[25]), relaxation delay, D_1 = 2 s, delay D_2 = 2.5 μs; 90° pulse, 8.7 μs; acquisition time, 1794 ms; sweep width in F_1 and F_2, 2283.13 Hz; size, 4K; 36 acquisitions, 512 increments; zero-filling up to 1K in F_1 and apodization with a squared $\pi/3$ shifted sine bell in both dimensions (measuring time, 19 h 26 min).

4. TOCSY (HOHAHA) Spectrum: sequence; D_1–90°–t_1–MLEV17-t_2; relaxation delay, D_1 = 2.0 s; mixing time for MLEV-17 (10.4 kHz), 10.4 ms; 90° pulse, 27.0 μs; acquisition time, 405.50 ms; sweep width in F_1 and F_2, 5050.50 Hz; size 2K; 16 acquisitions, 256 increments; zero-filling up to 512 W in F_1 and apodization with a squared $\pi/2$ shifted sine bell in both dimensions (measuring time, 2 h 47 min).

5. NOESY Spectra: sequence; D_1–90°–t_1–90°–τ_{mix}–90°–t_2; relaxation delay, D_1 = 2 s; mixing times, τ_{mix} = 150, 200, 300, 500, 600, 800, 1200, and 2000 ms; 90° pulse, 10.8 μs; acquisition time, 405.50 ms; sweep width in F_1 and F_2, 5050.50 Hz; size 2K; 56 acquisitions, 384 increments; single zero-filling in F_1 and apodization with a squared $\pi/2$ shifted sine bell in both dimensions (measuring time, 18 h 06 min, for τ_{mix} = 600 ms).

6. ^{1}H,^{13}C HMBC Spectrum: sequence, D_1–90°(^{1}H)–D_2–90°(^{13}C)–D_4–90°(^{13}C)–t_1/2–180°(^{1}H)–t_1/2–90°(^{13}C)–t_2(^{1}H); relaxation delay, D_1 = 2 s, D_2 = 3.57 ms, D_4 = 60 ms; 90° pulse, 10.5 μs (^{1}H), 11.9 μs (^{13}C); acquisition time, 405.50 ms; sweep width in F_1, 18 867.92 Hz, and in F_2, 5050.50 Hz; size, 2K; 64 acquisitions, 512 increments, zero-filling up to 1K in F_1 and apodization with a squared $\pi/2$ shifted sine bell in both dimensions. The spectrum was recorded and processed phase sensitive, followed by a magnitude calculation in the F_2 dimension; t_1-ridges were eliminated by subtracting coadded rows of a region without cross peaks from the whole 2D matrix, using the *Aurelia* program (measuring time, 22 h 28 min).

7. ^{1}H,^{13}C HMQC Spectrum: sequence; D_1-BIRD[26]-D_4–90°(^{1}H)–D_2–90°(^{13}C)–t_1/2–180°(^{1}H)–t_1/2–90°(^{13}C)–D_2–t_2(^{1}H), GARP[27] decoupling; relaxation delay, D_1 = 353.66 ms, D_2 = 3.57 ms, D_4 = 360.0 ms; 90° pulse, 10.1 μs (^{1}H), 11.9 μs (^{13}C); acquisition time, 202.75 ms; sweep width in F_1 18 867.92 Hz and in F_2 5050.50 Hz; size, 1K, 8 acquisitions, 128 increments; double zero-filling in F_1 and apodization with a squared $\pi/2$ shifted sine bell in both dimensions. t_1 ridges were eliminated by subtracting coadded rows of a region without cross peaks from the whole 2D matrix, using the *Aurelia* program (measuring time, 16 min).

Acknowledgment. We gratefully acknowledge for financial support the Deutsche Forschungsgemeinschaft, the Fonds der Chemischen Industrie for fellowships to M.R. and M.K., and the Fullbright Commission for a research award to D.F.M. We are indebted to Professor Dr. H. Kessler (Technische Universität München) for giving us the opportunity to work with his NMR facilities and to Professor Dr. D. Hoppe (Universität Kiel) who provided us with a sample of **1**.

Registry No. 1, 139609-21-5.

(24) Bodenhausen, G.; Vold, R. L.; Vold, R. R. *J. Magn. Reson.* **1980**, *37*, 93–103.
(25) Griesinger, C. Ph.D. Thesis, Frankfurt/Main, 1986.
(26) Garbow, J. R.; Weitekamp, D. P.; Pines, A *Chem. Phys. Lett.* **1982**, *93*, 504–509.
(27) Shaka, A.; Barker, P. B.; Freeman, R. *J. Magn. Reson.* **1985**, *64*, 547–552.